Bimodality in the Spatial Segment Density Distribution of Gaussian Chains

H. W. H. M. Janszen*

Faculty of Chemical Technology, University of Twente, P.O. Box 217, 7500 AE Enschede, The Netherlands

T. A. Tervoort

Centre of Polymer and Composites, Faculty of Chemical Engineering and Chemistry, Eindhoven University of Technology, P.O. Box 513, 5600 MB Eindhoven, The Netherlands

P. Cifra

Polymer Institute, Slovak Academy of Sciences, 842 36 Bratislava, Slovakia

Received July 31, 1995; Revised Manuscript Received April 22, 1996[⊗]

ABSTRACT: Investigation of the spatial segment density distribution (SSDD) of a Gaussian coil, generated using an off-lattice Monte Carlo method, revealed detailed information about the instantaneous shape. This information is used to compare shape models based on the principal components of the radius of gyration with an analysis in terms of block copolymer shape employing characteristic separation parameters. To speed up an accurate analysis, an analytical procedure for calculating both eigenvalues and -vectors of the radius of gyration tensor is developed. The observed averaged shapes are essentially bimodal (dumbbell-like) and do not depend on chain length. The numerical results confirm that an ideal homopolymer is to a large extent segregated into two equal parts. The influences of the left and right parts of a chain on the total shape are presented. These results, together with the evaluation of the density of special segments and the distribution of the separation angle between the parts, reveal the approximation inherent to the biellipsoidal model (BEM) and explain why the SSDD results and the BEM are not compatible. Also, an average arrowhead-like shape (as predicted by the BEM) is not observed. A suggestion of the idea can be made visible, but only after artificial averaging.

1. Introduction

The shape of linear polymer coils is relevant for various important physical properties, in particular in the theories of viscosity of dilute and concentrated polymer solutions and of polymer melts,[1] especially when dealing with processes with time scales shorter than the largest relaxation time of the Rouse spectrum.[2] Also, in long time scale processes, for example viscous flow, taking into account the aspherical shape of polymer chains can lead to a better fit between theory and experimental results.[3,4] Therefore, the averaged shape of linear polymers deserves an accurate characterization.

However, polymer molecules possess an almost infinite variety of chain conformations, which makes it impossible to describe their shape in terms of a simple geometrical form. Instead, all conformations together contribute to a "shape distribution". In general, characterization of these contributions is not feasible, which makes it necessary to characterize an "average shape" of a chain using an appropriate shape measure.[3]

Normally, the segment distributions for long chains are examined as an average over all possible orientations in space. The obtained segment distribution around the center of mass is therefore necessarily spherical in almost all theories of polymer properties in dilute solution.[5−9] In this case the distribution function of the radius of gyration and its orthogonal components is considered to be the satisfactory description of chain statistics. Many efforts have been made to characterize and approximate these size parameters.[10−14]

Kuhn[15] was the first to draw attention to the strong asymmetry of the random flight chain. Subsequently, Šolc and Stockmayer[3,16,17] illustrated that the average *instantaneous* shape of a polymer coil without orientational averaging is far from spherical. In their work, the eigenvalues of the gyration tensor were introduced as a shape measure and the distribution functions for linear combinations of the orthogonal components of this tensor were analyzed. The individual principal components were estimated by simulation techniques. The so obtained shape is profoundly asymmetric, regardless of the measure used for its quantitative description. This finds its origin in the infinite variety of irregular conformations, of which only a few possess symmetry elements.[16−19]

The first approximation of the segment density of a polymer coil was obtained by the introduction of the ellipsoidal model (EM) by Šolc, Gobush, and Stockmayer,[20] where an ellipsoidal shape was assigned to a polymer coil consistent with the triplet of the principal components of the gyration tensor. Eichinger and Wei[18,19,21] explored several distribution functions such as the simultaneous probability function of the eigenvalues using highly advanced analytical and numerical techniques. So far, the eigenvalues of the gyration tensor have resisted all attempts of an analytical treatment.[22]

Tanaka, Kotaka, and Inagaki[24] analyzed the shape of diblock copolymers by introducing parameters, like the separation angle θ between the blocks (see section 2). Later, on the basis of this work, Bendler and Šolc[23,39] introduced the biellipsoidal model (BEM) to investigate the effects of A−B incompatibility on the molecular shape in block copolymers. This model was based on the assumption that the blocks, having distinct chemical structures, deserve a separate description. The shape of each block was characterized by a single ellipsoid, joined together at their end segments and allowed to

[⊗] Abstract published in *Advance ACS Abstracts,* July 1, 1996.

S0024-9297(95)01114-4 CCC: $12.00

pivot around their common bonding point. The model agrees with the previous established theories[24−27] and shows that the segregation effects occurring in diblock copolymers as well as in homopolymers are well described by the separation angle θ between the blocks. In their study, it was concluded that the average conformation of homopolymers as well as block copolymers is most probably arrowhead-like. They also concluded that the BEM is a better shape model than the EM since it can be considered as the right step in a hypothetical hierarchy of models.[3,17]

In all models mentioned so far, the shape of a polymer was described by a small set of parameters, therefore leading to a limited image of the shape. More detailed information can be obtained by evaluating the spatial density distribution of all segments collectively. Unfortunately, this so-called "spatial segment density distribution" (SSDD), unlike the one for the end-to-end vector, does not reduce to a simple mathematical form without rigorous approximations, not even in the limit of infinite long chains,[28] so analytical treatment at this stage is not feasible. A first attempt to describe the SSDD was performed by Rubin and Mazur[1] by investigating the 3D density distribution of random walks and self-avoiding random walks in the principal axis system of the gyration tensor. By plotting histograms of the density projected along the three principal axes, it was shown that the segment density along the "longest" axis has a plateau. This line was followed by Theodorou and Suter,[29] who studied the influence of chain length and tacticity on the spatial segment density of an unperturbed polymer, polypropylene, using the rotational isomeric scheme concept (RIS).[30] Detailed information about the SSDD was obtained by using 3D plots. It was shown that the instantaneous shape of this polymer is essentially bimodal, even for long chains. The shape anisotropy was characterized by introducing new shape parameters like asphericity and acylindricity. More recently, analytical and simulation results of the asphericity and acylindricity and related shape parameters were also described.[22] Recently, the shape of the diblock was investigated by MC simulations in terms of a center monomer−arbitrary monomer correlation[31] and a dumbbell-like segregated shape was reported. However, the spatial segment density distributions obtained in these studies did not indicate any presence of an average arrowhead-like shape, as predicted by the BEM from Bendler et al.[23,39]

In this paper we will investigate the impact of different chain lengths on the shape of Gaussian chains to locate features general to all chains by the use of Monte Carlo simulation techniques. Furthermore, we will monitor the segregation effects and trace the relative position of the middle and end segments in the total distribution. Also we will pay attention to the question of compatibility between the detailed SSDD description and the above mentioned model.

2. Shape Models

To visualize the average instantaneous shape of a polymer molecule, orientational averaging needs to be avoided. This can be realized by taking the eigensystem of the gyration tensor of a chain as a frame of reference. For an individual chain with all segments possessing equal mass and the center of gravity placed on the origin, this gyration tensor[29] is defined as the average of the dyad $\mathbf{s}_i\mathbf{s}_i^{\mathrm{T}}$:

$$\mathbf{S} \equiv \frac{1}{N}\sum_{i=1}^{N}\mathbf{s}_i\mathbf{s}_i^{\mathrm{T}} = \begin{bmatrix} \overline{x^2} & \overline{xy} & \overline{xz} \\ \overline{xy} & \overline{y^2} & \overline{yz} \\ \overline{xz} & \overline{yz} & \overline{z^2} \end{bmatrix} \tag{1}$$

where $\mathbf{s}_i$ stands for the vector from the center of gravity of the chain to the ith segment. The overbar denotes averaging over all chain segments. The eigenvalues are assigned to $\overline{X^2}$, $\overline{Y^2}$, $\overline{Z^2}$, such that $\overline{X^2} \geq \overline{Y^2} \geq \overline{Z^2}$. Using the corresponding eigenvectors, transformation of the chain coordinates to its principal axis system will diagonalize $\mathbf{S}$ to $\mathbf{S}_{\mathrm{D}} = \mathrm{diag}(\overline{X^2},\overline{Y^2},\overline{Z^2})$. The squared radius of gyration, s^2, is equal to the trace of this tensor.

The eigenvalues thus characterize the asymmetry of a polymer chain. A first approximation to the SSDD can now be obtained by assuming a 3-dimensional Gaussian distribution where size and shape are dictated by the principal components of the gyration tensor, resulting in an ensemble of ellipsoidal smooth density clouds, called the ellipsoidal model (EM).[3,20,23]

A more detailed description of a coil shape is offered by studies of block copolymers,[23,24] recognizing that a polymer chain actually consists of two half-chains to be treated as two individual interpenetrating diblocks with zero interaction.

Parameters, characterizing the shape, were introduced by Tanaka et al.[24] and Bendler et al.:[23]

$$\gamma = \frac{\langle s^2\rangle_{\mathrm{K}}}{\langle s^2\rangle_{\mathrm{H\text{-}K}}} \qquad \gamma_{\mathrm{R}} = \frac{\langle R^2\rangle_{\mathrm{K}}}{\langle R^2\rangle_{\mathrm{H\text{-}K}}} \tag{2}$$

$$\sigma = \frac{\langle G^2\rangle}{2(\langle s^2\rangle_{\mathrm{H\text{-}A}} + \langle s^2\rangle_{\mathrm{H\text{-}B}})} \qquad \mathrm{K} = \mathrm{A, B}$$

where $\langle s^2\rangle_{\mathrm{H\text{-}K}}$ is the mean square radius of gyration of a homopolymer molecule identical with the K block and exposed to the same environment as the "block copolymer" molecule, $\langle R^2\rangle_{\mathrm{H\text{-}K}}$ is the mean square end-to-end length of a homopolymer molecule identical with the K block and exposed to the same environment as the "block copolymer" molecule, and $\langle G^2\rangle$ is the mean square distance between the centers of gravity of each block. Also used are $\mathbf{G}_{\mathrm{K}}$, the vector from the joint bond to the center of gravity of block K, and $\langle G^2\rangle_{\mathrm{K}}$, the corresponding mean square distance. Another important quantity is the separation angle $\langle\theta\rangle$, defined as the mean angle between the vectors $\mathbf{G}_{\mathrm{A}}$ and $\mathbf{G}_{\mathrm{B}}$; see Figure 1. On the basis of values of the above mentioned parameters, especially $\langle\theta\rangle$, Bendler et al.[23,39] introduced the biellipsoidal model of a block copolymer (BEM). In this approach, each pair of blocks is represented by two ellipsoidal Gaussian segment clouds, calculated from the reduced square principal components.[20] The two blocks are then joined together by their end vectors, resulting in an average arrowhead-like shape for a polymer chain.[17] It was shown that the BEM gives a good description of the principal values for $\mathbf{S}$ of the complete polymer.[3,17,23]

The most detailed description of the instantaneous shape of a polymer chain is offered by the SSDD, where the density at a given point in the space, occupied by the molecule, comprises the contribution from each separate segment of the chain. This contribution is then represented by the frequency of occurrence of the segment in question within a volume element at a given point.[28] Although a suitable mathematical description

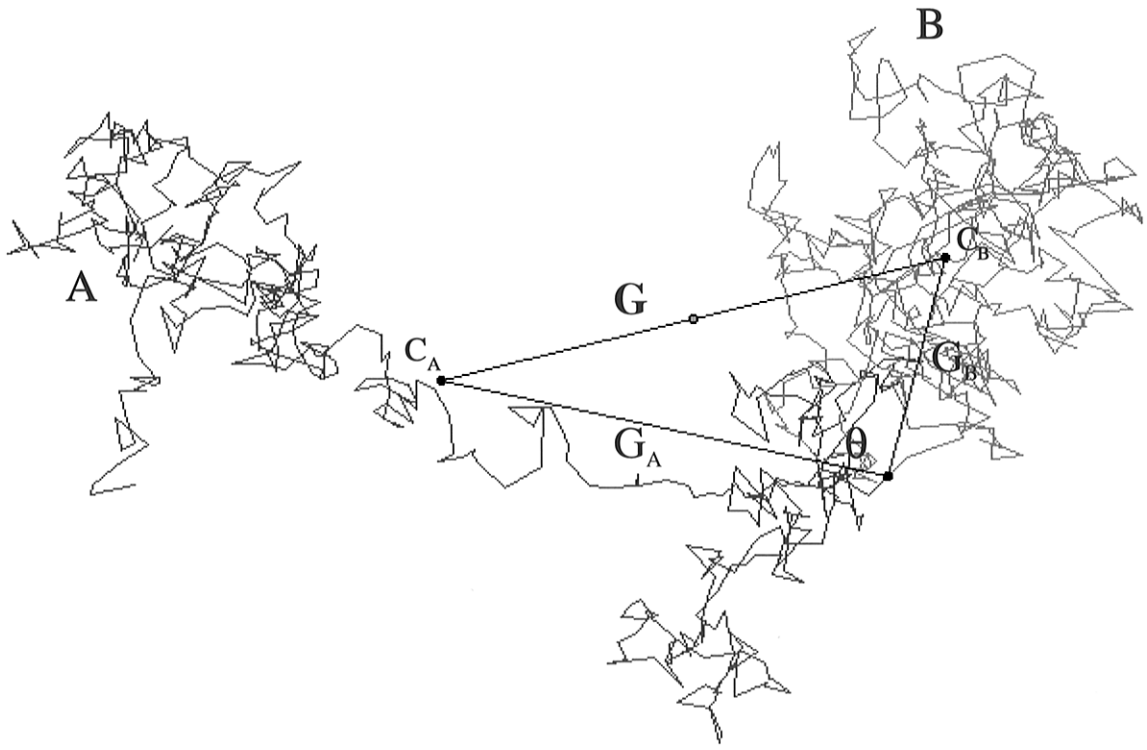

Figure 1. Separation vectors and parameters in an arbitrary configuration of an isolated AB block copolymer, where each block has a length of 500 segments. C_A and C_B represent the centers of gravity of the respective blocks.

of the distribution as described is not present, information about this density can still be obtained by using an appropriate simulation method.[32] Combining and averaging a sufficient large amount of conformations of a given chain will lead to an approximation of the desired distribution, giving very detailed information about the average shape.

3. Monte Carlo Techniques

As a starting point, the shape of a complete Gaussian chain was examined by calculating the SSDD for several chain lengths. This was done by numerical simulation experiments according to the following procedure.

First a chain of a given number of segments was generated,[32−34] from a multinormal Gaussian distribution with zero mean and variance of $\sigma^2 = {}^1/_3$ for each separate coordinate, resulting in a mean square bond length of $\langle l^2 \rangle = 1$. Then this chain was translated in such a way that its center of gravity was placed in the origin. Next the eigenvalues as well as the eigenvectors of the gyration tensor **S** of this particular chain were analytically computed, after which the chain was transformed to the obtained eigensystem. Following the approach of Theodorou and Suter,[29] the chain coordinates were stored in a 3D lattice block of appropriate size, with the center of gravity at the origin and having edges parallel to the principal axes. This lattice block was subdivided into a grid of 80 × 50 × 30 cells, where each cell is a cube with a volume of $(R/20)^3$, where $R \equiv \langle R^2 \rangle_0^{1/2}$ is the averaged length of the end-to-end vector. So the size of each distribution of arbitrary chain length is scaled to a volume of $\langle R^2 \rangle^{3/2}$. For the Gaussian chains the scaling of the lattice blocks was performed with the exact analytical value of the squared length of the end-to-end vector **R**.

These steps were repeated until a sample of sufficient size was generated, after which a confident estimation of the spatial segment density distribution was obtained by simply counting and/or averaging the segments in the cells of the lattice block.[32] Also, to speed up the convergence of the simulation, this distribution was symmetrized over all octants around the origin of the lattice block. To avoid time-consuming iteration processes and inaccurate results due to ill-conditioned matrices during the analysis, not only the eigenvalues but also the eigenvectors of any individual gyration tensor were analytically solved and afterward averaged. With the absence of a general solution for the eigenvector problem of this symmetric tensor, an analytical method was derived which is presented in Appendixes A and B.

Once having obtained the estimated spatial distribution of a given sample, it is also possible to deduce from this sample quantities like the maximum or average density of a chain. These densities were approximated by

$$\rho_{\max} \equiv \frac{\max_i \langle M \rangle_i}{V_{\text{cell}}}; \qquad \rho_{\text{av}} \equiv \frac{\sum_i{}' \langle M \rangle_i}{V_{\text{cell}} * L}; \qquad V_{\text{cell}} = \left(\frac{R}{20}\right)^3 \qquad R \equiv \langle R^2 \rangle^{1/2} \quad (3)$$

where $\sum'$ is defined as the summation over all **filled** cells, $\langle M \rangle$ as the average number of segments in the ith cell, and L as the number of filled cells.

Shape parameters were calculated in the following way: The chains, having a certain length of $N = 2n$ segments, were considered to be divided in two equal parts consisting of n segments. The desired size of the vectors $\mathbf{G}_A$, $\mathbf{G}_B$, and **G** and the angle θ (see Figure 1) were then computed for each chain and averaged over all configurations. Because of the use of an even number of segments the joint segment was replaced by a joint bond with its reference point in the middle of the vector $\mathbf{r}_{n,n+1}$.

The number of possible intrachain interactions was also studied by calculating the segmental contacts. For

Table 1. Principal Values for Several Models with Uncorrelated Bonds: Unrestricted Random Walks on Cubic Lattice, Gaussian, and Freely Jointed Chains (f.j.c.)

ref	type	N	$\langle\overline{X^2}\rangle/\langle\overline{Z^2}\rangle$	$\langle\overline{Y^2}\rangle/\langle\overline{Z^2}\rangle$
Šolc[16,17]	RW, ideal	50	11.8	2.7
Šolc[16,17]	cubic lattice	100	11.7	2.7
Wei[21]	Gaussian	29	12.41	3.11
Koyama[37]	analytical f.j.c.	$\rightarrow\infty$	10.6	2.5
this study	Gaussian	1000	12.03	2.72

this purpose, all distances between all segments of a chain were calculated, with the exception of direct neighbors in the chain. A contact was detected if this distance was smaller than $R_{\text{critical}} = 1$. A distinction was made between interior (within one half of a chain) and hetero contacts (between two halves of a chain).

The chains were examined for a polymerization degree (chain length) varying between $N = 10$ and 1000 segments. In each experiment a sample of 50 000 chains was generated, which should result in a relative standard error[35] of $\epsilon \cong 0.003$ for the second moment of **R**, independent of the chain length. The estimated values obtained from the simulations were in good agreement with the exact values within this error. The values of the other calculated quantities, in particular the principal values, given in Table 1, were also in agreement with earlier results[16,21,22] possessing relative standard errors of the same order as those for the end-to-end vector. As could be expected,[18,19,21] after the analytical deduction of the principal values of the gyration tensor of each separate chain of the samples, we never observed any multiple eigenvalues for the Gaussian model. So all configurations in our samples are basically asymmetric.

The ratio of the lattice block size was in good accordance with the ratio of the second moments of the spans calculated by Rubin[36] for unrestricted RW's.

The parameters, characterizing the shape of diblock copolymers, were observed to satisfy the additivity rules for AB diblock copolymers, where homopolymer A is the left part and B is the right part of the chain.

$$\langle s^2\rangle = \frac{1}{2}\langle s^2\rangle_A + \frac{1}{2}\langle s^2\rangle_B + \frac{1}{4}\langle G^2\rangle \qquad (4)$$

$$\langle G^2\rangle = \langle G^2\rangle_A + \langle G^2\rangle_B - 2\langle G_A G_B \cos\theta\rangle$$

4. Results and Discussion

1. Coil Shape Characteristics. To obtain an impression of the average shape of a chain, cross-sections through the obtained blocks, in particular along the principal axes, are depicted in Figure 2a,b. It is observed that, with exceptions for small N ($N \leq 10$), the average instantaneous *scaled* shapes are all similar and of equal size. The characteristics of this scaled shape are depicted in Figure 2a,b for a chain length of $N = 40$ segments. In these figures, the densities are presented as the fractions of the observed maximum segment density of the respective sample. For $N < 10$, the chosen resolution is too high, because the segment size becomes much larger than the cell size.

The intersections taken along the $X-Y$ plane through the principal axes ($Z = 0$ and $Y = 0$) and the 3D projection of an octant of the SSDD (Figure 2a,b) show that the contour or extent of the average shape of a Gaussian chain, formed by its lower density domains, is ellipsoidal. However, it can be observed that the SSDD itself has a dumbbell-like shape with two maxima, located along the longest principal axis at a position of $\pm 0.3R$ from the origin. The existence of a possible average arrowhead-like shape cannot be observed in these pictures, although it is predicted by the BEM also for homopolymers.

Normalized projections of the total density on the principal axes, similar to those by Rubin et al.[1] and later by Theodorou et al.[29] show that the density along the longest axis, near the origin, is never actually flat; see Figure 3a. So, we do not confirm the observations made by Rubin and Mazur,[1] but our results for Gaussian chains are in accordance with the results by Theodorou and Suter[29] for polypropylene. However, the strong separation between domains, as observed for polypropylene, is not present here. A better view of the density behavior is obtained by plotting the density profile just along the X-axis, see Figure 3b. From this plot a local minimum at the origin is clearly observed, although it has a density value of only 5% less than the maximum density value. This might be the reason why it was not noticed before by Rubin et al.[1]

All obtained shapes possess an equal size. Because they are scaled as described in part 3, their size has to be proportional with $\langle R^2\rangle^{3/2} = (N-1)^{3/2}$. The scaling properties of a chain are also demonstrated by plotting the maximum and average densities from the samples against the number of chain segments, as shown in Figure 4. The slope of $-1/2$ in this figure indicates that the obtained approximated values for the densities scale with the chain length as

$$\rho \propto \frac{N}{V_{\text{shape}}} \propto \frac{N}{{}^4/_3\pi\langle R^2\rangle^{3/2}} \propto N^{-1/2} \qquad \text{for large } N \quad (5)$$

The values for the maximum density are remarkably close to the analytical result of Debye and Bueche:[5]

$$\rho_{\max}^{\text{DB}} = \left(\frac{2}{N}\right)^{1/2}\left(\frac{9}{\pi C_N l^2}\right)^{3/2} \qquad N \rightarrow \infty \qquad (6)$$

which, however, they obtained at the center of an orientionally averaged spherical symmetric distribution.

The scaling properties of the size and the similarity of the shape point out that the instantaneous shapes of Gaussian and freely jointed chains have a universal character. The normalized projections of density of the chains are, like the SSDD, indistinguishable for different chain lengths. This outcome is not a surprise, because the principal values, by definition also based on the position of all segments, also have a constant ratio for larger N, in our case from $N \geq 10$.

However, it should be mentioned that the tails of the distribution, formed by the areas with densities less than 1% of the maximum, tend to spread out with larger N, which means that the distribution becomes broader for longer polymers. However, the effects on the total average distribution are negligible.

The values obtained for the shape parameters and the scaled averaged squared length of the vectors are also independent of chain length for $N \geq 10$. They are presented in Table 2, together with the relative standard errors. Due to the absence of any excluded volume interactions in our model, the expansion parameters γ and γ_R give a trivial value of unity. Our calculations of the shape parameters for the Gaussian chains match those of the pivoting approach.[23] The separation parameter σ has a unity value, corresponding with a separation angle of $\langle\theta\rangle = 90°$, being in agreement with the earlier results[23,24] for homopolymers at the Θ state. So we observe that Gaussian chains are indeed to a

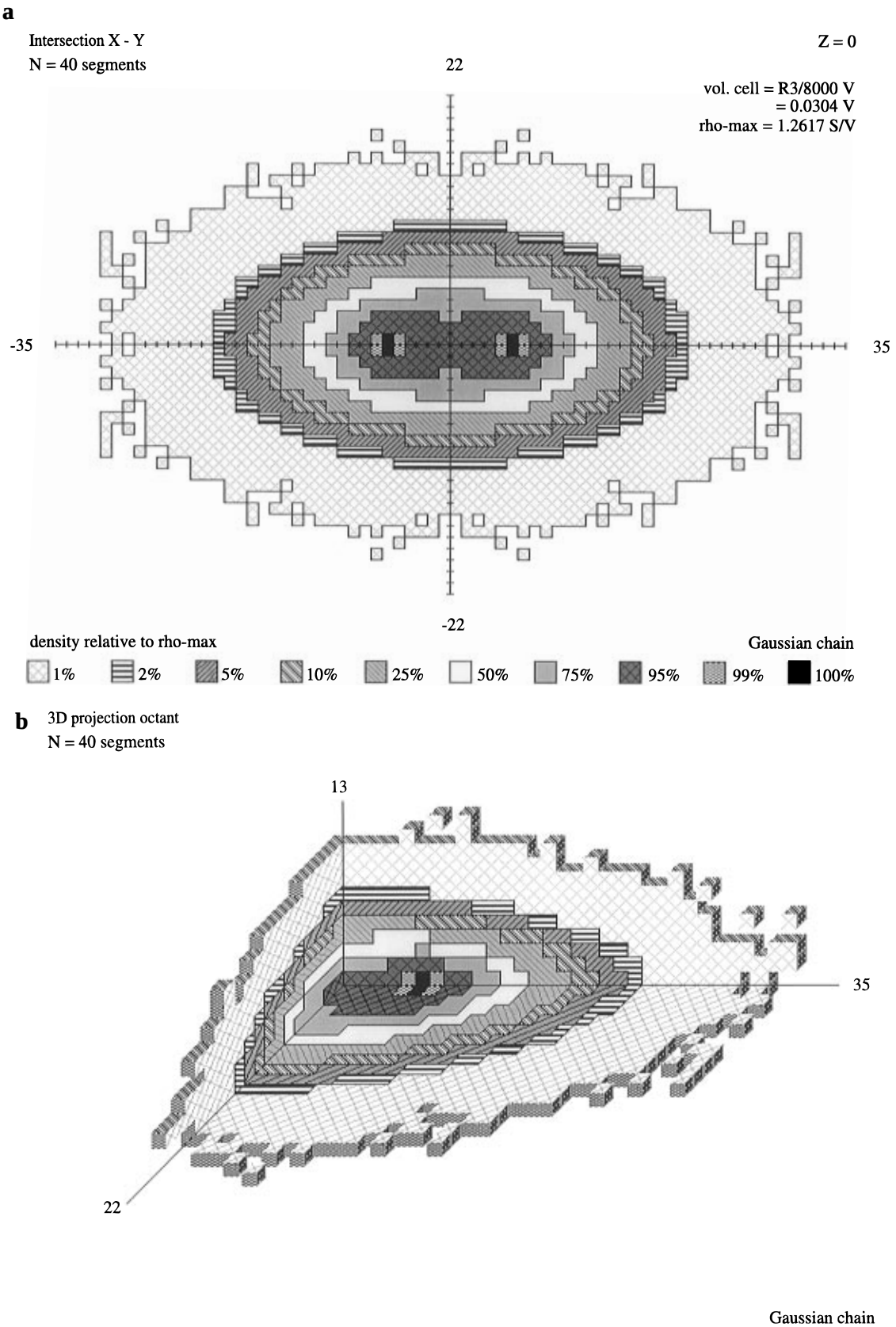

Figure 2. Spatial segment density distribution of a Gaussian chain with a length of 40 segments, as a fraction of the maximum segment density of a chain, transformed to the eigensystem of its gyration tensor: (a) intersection $X-Y$ plane; (b) 3D projection of an octant of the distribution.

large extent segregated in the sense as described earlier. However, we should realize that *the computing and averaging of the separation parameters is, by the way they are defined, independent of any chosen representation of the average shape. These results therefore do not imply the existence of an average arrowhead-like shape.*

We will show that typical values of the above mentioned parameters are compatible with a dumbbell-like shape. An average arrowhead-like shape can be visualized only by employing a special averaging procedure.

2. Compatibility of the Shape Models. It is shown by the results so far, that the existence of an

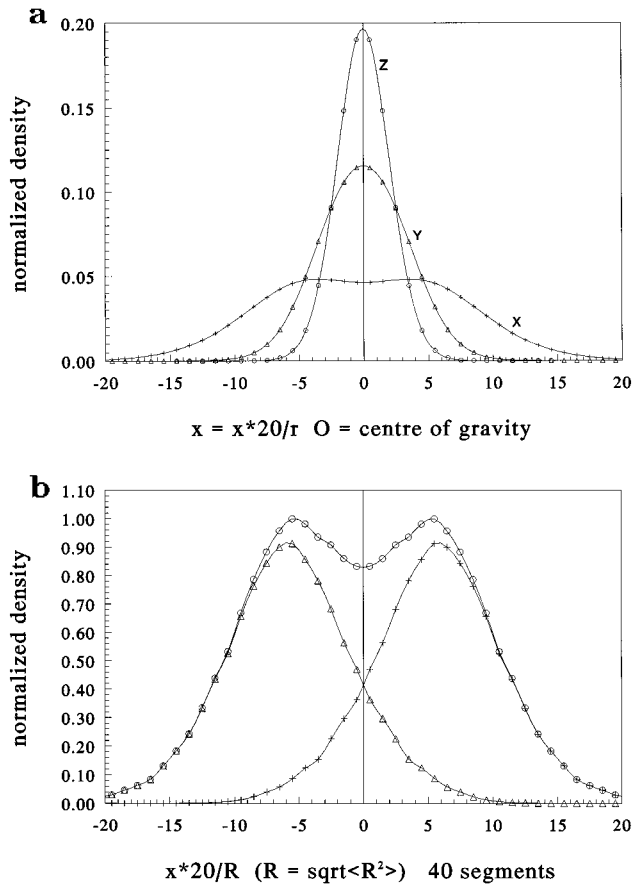

Figure 3. (a) Normalized projections of the total segment density on the three principal axes of the gyration tensor of a chain with 1000 segments. (b) Normalized segment density with respect to ρ_{max} along the X-axis, contribution of the chain halves to this density. Key: (+) left; (△) right; (○) total.

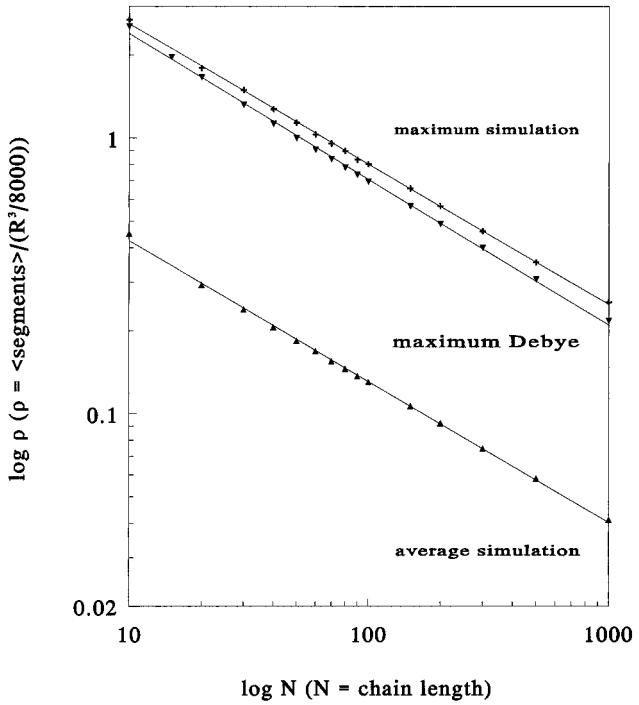

Figure 4. Maximum and averaged segment densities of a Gaussian chain for several chain lengths.

average arrowhead-like shape cannot be confirmed. Therefore, we have studied to what extent both shape models, i.e. SSDD and BEM, correspond to each other.

We also studied the distributions of any particular segment or a particular set of segments in the overall

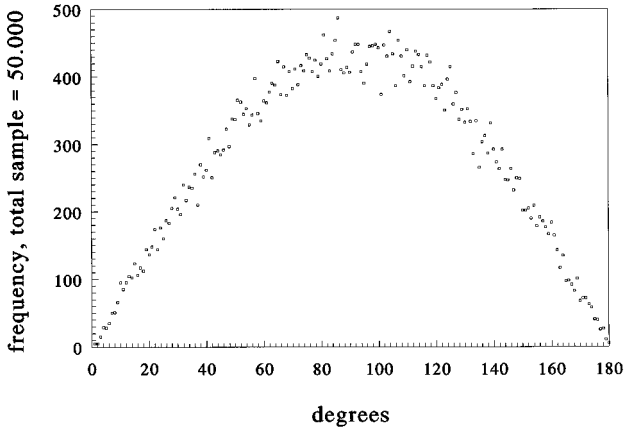

Figure 5. Distribution of the separation angle θ from a sample of 50 000 chains of a Gaussian chain with 1000 segments.

Table 2. Separation Parameters and Vectors

av params	Gaussian
$\gamma_{A/B}$	0.999
$\gamma_{R,A/B}$	1.000
σ	1.000
θ (deg)	90
Standard Errors (Relative)	
$s(\gamma_K)$	±0.002
$s(\gamma_{RK})$	±0.003
$s(\sigma)$	±0.004
$s(\theta)$ rel	±0.002
Averaged Vectors Scaled Length	
$\langle G^2\rangle/\langle R^2\rangle$	$\langle G_K^2\rangle/\langle R^2\rangle$
0.335	0.168

spatial segment distribution. Because the basic ideas of the BEM depend on the position of the end segments, it is of interest to locate the end *and* middle segments, where the last ones have to be considered as the joined ends of the two imaginary separate blocks.

The end segments of Gaussian chains were found to be dispersed over the whole distribution, therefore their contribution to the total density in each point is negligible (<1% of ρ_{max}). When considering the distribution relative to its own density maximum, it is observed that the highest densities are found in two spherical domains, both with a radius of $0.12R$. The centers of these domains are symmetrically situated on the longest axis on a relative position of $0.5R$ from the origin. However, only 8% of all end segments are found to occur in these spheres. *Therefore, the assumption*[23] *of having the ends near the tips of the cigars is not correct although it is a central assumption of the BEM.* The ellipsoids are joined together at the chain ends,[39] or as stated elsewhere, $\mathbf{G}_A$ and $\mathbf{G}_B$ are fixed relative to the principal axes of the respective blocks;[23] therefore connection of the two blocks as described is problematic.

The distribution of the middle segments, given the possible location of the joint bond, is more compact. These segments are apparently found in a sphere centered around the center of gravity, with a density maximum in this center. The middle segments contribute about 25% to the total density in this area.

It was also found that the high-density domains are mainly formed by the segments at $^1/_4$ or $^3/_4$ of the chain. When the positions of centers of gravity of the separate blocks were traced, it was found that the most likely position of these centers matches very well these maxima in the overall shape pictures. So we may presume that the density maxima of the SSDD of the

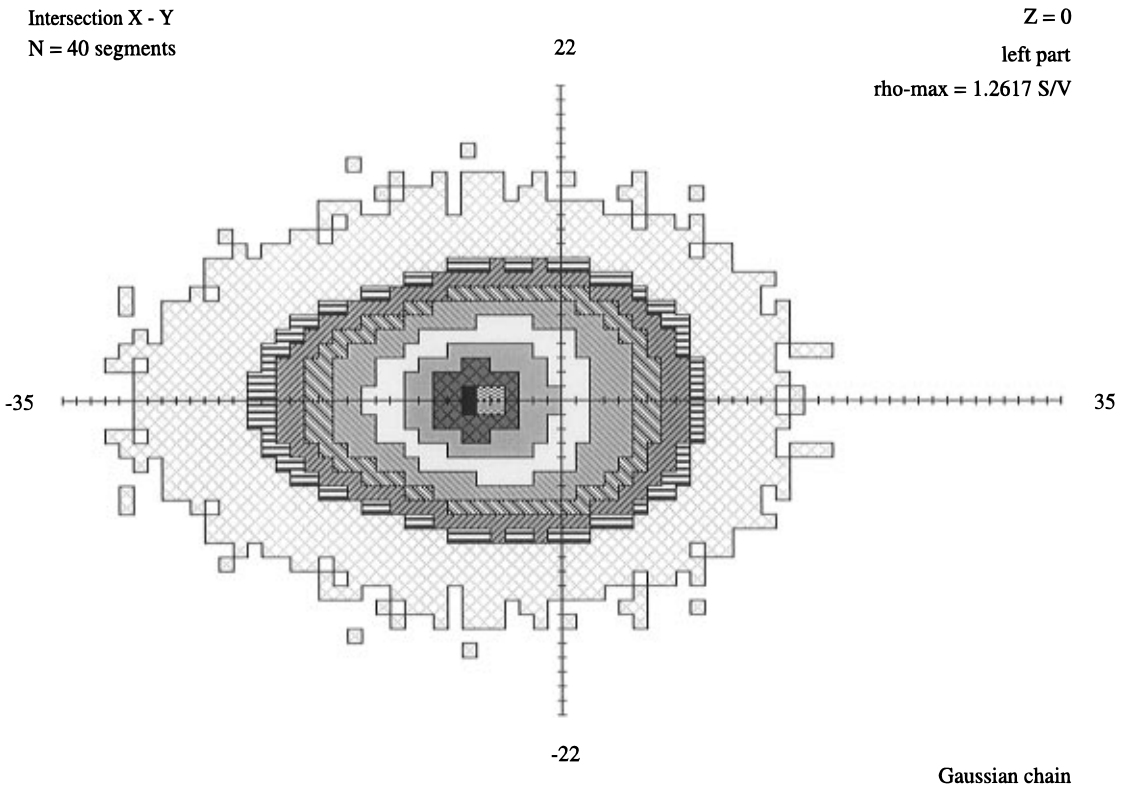

Figure 6. $X-Y$ plane intersection of the segment density of a left block of a Gaussian chain with 40 segments after separation of the sample according to the centers of gravity criterion.

whole chain (Figure 2a) to a large extent exist out of the centers of gravity of the left and right part of the chain (Figure 6).

When these results are combined with the averaged distances between the centers of gravity (Table 2), being relative short, it becomes clear that the gravity centers of the blocks and joint bond all lie within a sphere with a radius of $0.3R$ around the origin. It is, therefore, quite possible to find an averaged separation angle of $\langle\theta\rangle = 90°$ in the obtained conformations, without observing an average arrowhead-like shape.

The separation angle also deserves some attention. At first sight, the relative standard error of the *estimate* of θ given in Table 2 may look acceptable. Actually, due to the followed statistical procedure, this quantity is related not only to the variance of θ but also to the sample size. This error is diminishing with increasing sample size. However, the distribution of θ has a large variance of the same order as the end-to-end distance. Examining this distribution for our samples leads to a broad curve with a range of $0-180°$ with an expectation value of $\langle\theta\rangle = 90°$, which is presented in Figure 5. Then it can be observed that the angle θ has a frequency function proportional with $\sin(\theta)$, which is actually a consequence of the fact that two parts of a chain are mutually independent of each other.[40]

Next we have examined the impact of the segregation effects on the overall average instantaneous shape. With the knowledge that a chain actually can be regarded as consisting of two (equal) parts, we have studied the individual contribution of each of the two blocks to the total spatial distribution of the shape. To make this possible, the original concept was slightly modified. After a sample of complete chains was produced, each chain half was stored separately in a distinct left or right block, to obtain a proper separation. The most difficult part in this process was to find an appropriate selection criterion to decide which part of the chain is left or right, after translating the chain to its eigensystem.

The first results for separation were obtained by using criteria where the X-coordinates of certain segments were compared, like the first with the last segment or the two middle segments (N = even). However, after tracing and plotting the positions of the centers of gravity of the blocks, at least 30% of these centers was found to occur in the opposite half of the distribution. Using the X-coordinates of both centers of gravity of each block as criterion resulted in a better separation, and the shape of each block became visible. In this way obtained distributions are necessarily asymmetric relative to the $Y-Z$ plane, so the reflecting of the X-coordinates on this plane had to be canceled. From Figure 6 it is observed that the average shape of a separate block can be described as egg-shaped.

The segregation effect is depicted by the density plots along the X-axis; see Figure 3b. From this figure it is observed that the curves, representing the separate block contributions, are nearly Gaussian-shaped; only the outer tail is more stretched. This effect is caused by the fact that both blocks are not averaged and presented in their own eigensystem but are still submitted to the eigensystem of the whole chain. This introduces an additional orientational averaging effect. If the blocks are evaluated with respect to their own eigensystems, a dumbbell configuration emerges again. Thus, Gaussian chains are self-similar, as was also recognized by Bendler et al.[17,23]

However, a representation of the spatial segment density as proposed by Bendler and Šolc[23,39] is not possible. If one of the blocks would be represented with respect to its own eigensystem, then the other half of the chain is found to be pivoting around the junction point. Also, a block represented in its own eigensystem should again resemble a dumbbell instead of an ellipsoidal shape.

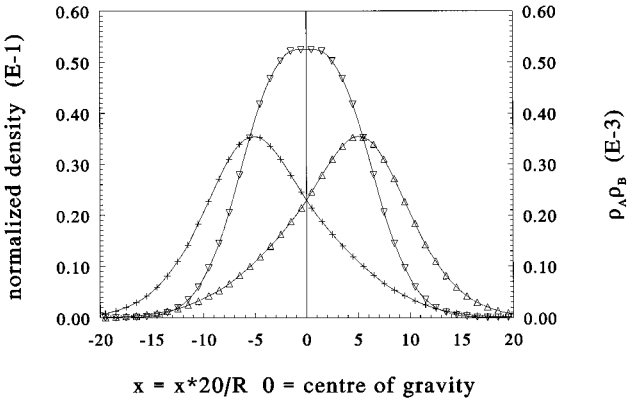

Figure 7. Locations of N_{AB} contacts, projected on the X-axis, where the degree of AB block overlap is presented as the product curve $\rho_A\rho_B$ for a chain with 40 segments. Key: (+) ρ_A; (△) ρ_B; (○) $\rho_A\rho_B$.

In fact the BEM holds a contradiction, giving *two* answers for the average shape which both must apply for one and the same homopolymer chain. The reason that the adoption of a Gaussian density for the separate blocks as defined by Bendler and Šolc[23] is a reasonable approximation is that both halves of the chains are not evaluated in their *own* eigensystem, but in the eigensystem of the *total* chain.

The principal problem with the BEM is that the averaging over many configurations, to obtain the shape of half-chains, was made separately for each of two half-chains. After joining the blocks, the obtained arrowhead-like "shape" is neither an individual configuration nor an average shape. To obtain an average shape, an appropriate reference frame for the total chain has to be chosen. So the instantaneous average shape of a chain should be evaluated with respect to the eigensystem of the total chain. In the BEM this would introduce an additional averaging over all possible rotations around the longer axis, after which the arrowhead-like shape would be lost.

Our conclusions are independently supported also by Rubin et al.[1] and Suter et al.[29] and for diblocks by Bassler et al.[31] who did not find the average arrowhead-like shape but support the dumbbell-like shape.

With respect to the shape it was already mentioned that a separation angle of $\theta = 90°$ does not imply an average arrowhead-like shape as predicted by the BEM. However, the arrowhead-like shape can actually be made visible as a 3D representation if we leave the original eigensystem concept and manipulate the samples by some artificial transformations. For each chain, the centers of gravity of both blocks have to be determined. The chain is then positioned in such way that these centers lay on the X-axis at equal distances from the origin. Subsequently, we rotate the chain along the X-axis, until the junction point is positioned in the $X-Y$ plane with positive Y. The average shape that arises shows a pronounced "arrowhead", in particular the average separation angle becomes visible; see Figure 8.

However, the so obtained segment density refers neither to the eigensystem of the whole chain nor to the eigensystems of the separate blocks. Representing the spatial distribution this way emphasizes the strong dependence of the obtained averaged shapes on the choice of the reference frame.[38]

We also want to state that the so obtained average shape is to a large extent dependent on the position of the junction point of the blocks. An estimation of the average shape of a chain should be based on the positions of *all* segments rather than on a certain special chosen segments.[16] Using the principal values of the gyration tensor guarantees that all segments contribute at an equal extent to the spatial density distribution.

Together with the calculation of the separation parameters the occurrences of intrasegmental contacts in the samples were also calculated, as defined in section

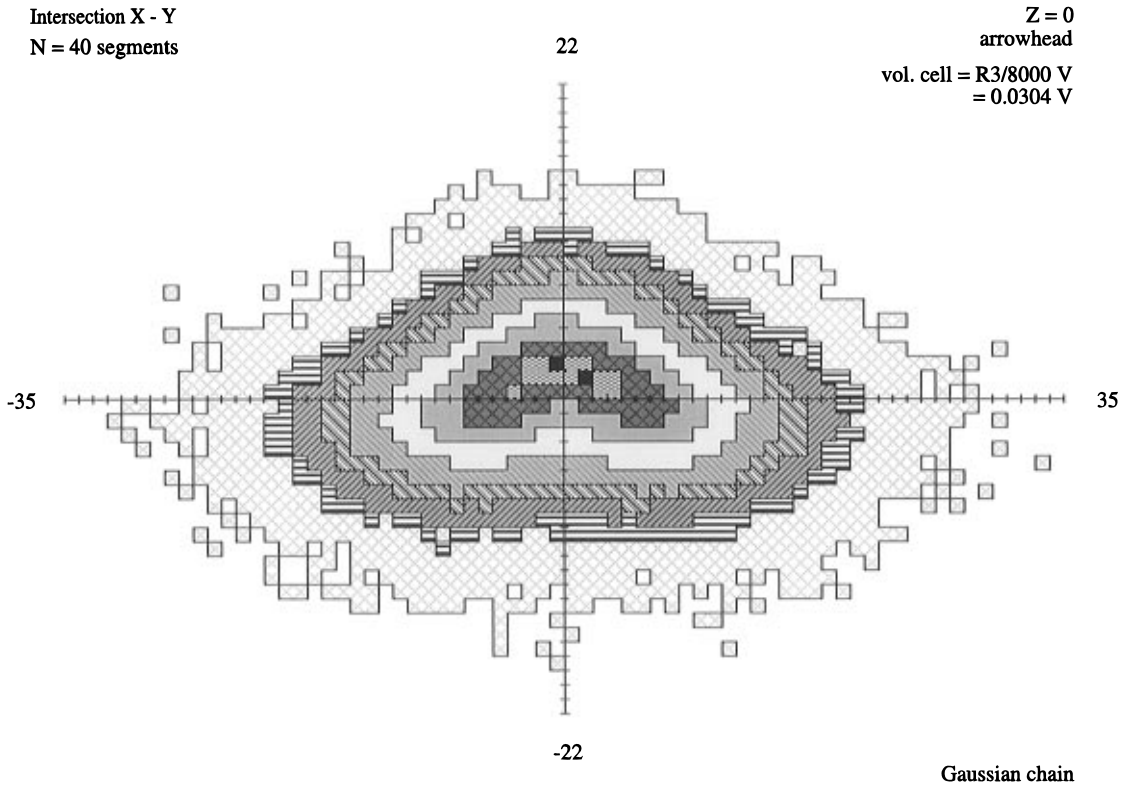

Figure 8. Averaged "arrowhead" shape representation of a Gaussian chain with 40 segments after rotation of the junction point into the $X-Y$ plane with positive Y.

Table 3. Number of Intrasegmental Contacts for Several Chain Lengths in a Radius of $R_{critical} = 1$ around All Segments, with the Exception of the Nearest Neighbors

	Gaussian		
$N = 2n$	N_C	N_{AB}	N_{AB}/N_C
10	1.022 44	0.360 40	0.3525
20	1.280 20	0.249 44	0.1948
30	1.379 36	0.205 54	0.1490
40	1.456 54	0.180 60	0.1240
50	1.502 44	0.160 46	0.1068
60	1.546 80	0.151 02	0.0976
70	1.561 40	0.140 02	0.0897
80	1.586 74	0.132 64	0.0836
90	1.606 80	0.127 68	0.0795
100	1.611 06	0.116 08	0.0721
150	1.663 40	0.093 92	0.0565
200	1.698 32	0.081 50	0.0480
300	1.756 48	0.065 64	0.0374
500	1.773 98	0.053 20	0.0300
1000	1.798 46	0.037 98	0.0211

2. The results are presented in Table 3; with N_c as total, N_{BB} and N_{AA} as interior, and N_{AB} as number of heterocontacts, then $N_C = N_{AA} + N_{BB} + N_{AB}$, since it can be assumed that $N_{AA} = N_{BB}$.

With exception for the fractions of N_{AB}/N_C the results are dependent on the chosen radius R_c. The trends in the Gaussian results confirm the earlier results:[25−27]

$$\frac{N_C}{R^3} \propto \rho_{av}{}^2 \propto \frac{1}{N} \tag{7}$$

Using the separation scheme, it is now possible to show where the integration takes place. In Figure 7 the locations of possible interpenetration are presented as projections in the sense as described in section 4.1. It is shown that the most likely heterocontacts are located in the $Y-Z$ plane at the origin, perpendicular on the X-axis, the longest principal axis.

5. Conclusions

It can be concluded that the instantaneous shape of an ideal flexible coil is best characterized as dumbbell-like or bimodal, while the span or extent of this shape is an ellipsoid. The shape of a Gaussian chain can be considered as "self-similar". This is based on the fact that splitting up every chain of a sample in equal parts and then reorganizing them according to the described principle result in shapes that are an exact copy of the original.

Besides all size, density, and other parameters like $\langle G^2 \rangle$ and $\langle G^2{}_k \rangle$, also the dimensions of the instantaneous shape fulfill the scaling laws. The bimodal character of the spatial segment density shape can be considered as universal, which makes the spatial segment density distribution as a shape measure quite useful.

The average arrowhead-like shape as predicted by the biellipsoidal model was not confirmed in our numerical simulations. The average simulation angle of 90°, describing the segregation of the two blocks, was shown to be consistent with a dumbbell-like shape of a homopolymer.

The Gaussian density profile used for the two blocks in the biellipsoidal model was shown to be a result of an additional orientational averaging introduced by evaluating the two blocks in the eigensystem of the *total* chain. Only by an artificial averaging method can an arrowhead-like shape be observed.

The "natural" segregation that occurs in Gaussian chains is an interesting characteristic, which seems to be responsible for the occurrence of the dumbbell-like shape.

Acknowledgment. With special thanks for Dr. P. Jonker, University of Twente, for his contribution to the eigenvalue evaluation and for Prof. Dr. Ir. H. E. H. Meijer, University of Eindhoven, for the financial support of the project.

Appendix A

Analytical Deduction of the Eigenvalues of the Gyration Tensor. Due to the symmetry of the gyration tensor **S**, it is always possible to deduce three real eigenvalues for the individual tensor, from the characteristic equation:

$$|\mathbf{S} - \lambda \mathbf{I}| = \lambda^3 - I_1\lambda^2 + I_2\lambda - I_3 = 0 \tag{A1}$$

with I_k as the invariants of the tensor, defined as

$$I_1 = \mathrm{tr}(\mathbf{S}) \tag{A2}$$

$$I_2 = \begin{vmatrix} \overline{x^2} & \overline{xy} \\ \overline{xy} & \overline{y^2} \end{vmatrix} + \begin{vmatrix} \overline{x^2} & \overline{xz} \\ \overline{xz} & \overline{z^2} \end{vmatrix} + \begin{vmatrix} \overline{y^2} & \overline{yz} \\ \overline{yz} & \overline{z^2} \end{vmatrix}$$

$$I_3 = \det(\mathbf{S})$$

Unfortunately, this equation is of the irreducible type.

This problem can be avoided by making the tensor traceless by substituting

$$\xi = \lambda - \frac{1}{3}I_1 \tag{A3}$$

Then the characteristic equation reads

$$\xi^3 + p\xi + q = 0 \tag{A4}$$

with $p = I_2 - (1/3){I_1}^2$ where $p < 0$ and $q = 1/3 I_1 I_2 - I_3 - (2/27){I_1}^3$.

The discriminant of this equation satisfies the inequality

$$4p^3 + 27q^2 < 0 \tag{A5}$$

After $\xi = r\cos(\varphi)$, r and φ real, $r > 0$, is substituted in the characteristic equation, the following result is obtained:

$$\frac{1}{4}r^3\cos(3\varphi) + r\left(\frac{3}{4}r^2 + p\right)\cos(\varphi) + q = 0 \tag{A6}$$

Choosing $r = 2\sqrt{-{}^1/_3 p}$, with (A5) gives

$$\cos(3\varphi) = -\frac{4q}{r^3} = \frac{9q}{2p\sqrt{-3p}} \tag{A7}$$

then

$$\xi_{1,2,3} = 2\sqrt{-\frac{1}{3}p}\,\cos\left(\varphi_1 + \frac{2}{3}k\pi\right) \qquad k = 0, \pm 1$$

with

$$\varphi_1 = \frac{1}{3}\arccos\left(\frac{9q}{2p\sqrt{-3p}}\right) \tag{A8}$$

After $\xi_{1,2,3}$ is substituted in (A3), $\lambda_{1,2,3}$ is obtained. See also Koyama[37] for a comparable method.

Appendix B

Analytical Deduction of the Eigenvectors of the Gyration Tensor. Because the tensor is symmetric, there always exists a complete set of three orthogonal eigenvectors. When the eigenvalues are known, the corresponding eigenvectors can easily be deduced by solving the set of equations for each eigenvalue: $S\mathbf{x} = \lambda\mathbf{x}$, after the substitution of

$$\mathbf{x} = \begin{bmatrix} x_1 \\ x_2 \\ x_3 \end{bmatrix} = \begin{bmatrix} r\cos(\theta)\cos(\varphi) \\ r\cos(\theta)\sin(\varphi) \\ r\sin(\theta) \end{bmatrix} \tag{B1}$$

With one degree of freedom available for these parameters, the most suitable choice is to set $r = 1$, which makes the eigenvector set orthonormal. Then a general analytical solution for φ and θ, with some simple exceptions, is obtained.

General solution for φ and θ:

$$\text{tg}\,\varphi = \frac{\overline{yz}\,\overline{x^2} - \overline{xz}\,\overline{xy} - \overline{yz}\,\lambda}{\overline{xz}\,\overline{y^2} - \overline{yz}\,\overline{xy} - \overline{xz}\,\lambda}$$

$$\text{tg}\,\theta = \frac{\overline{xz}\cos\varphi + \overline{yz}\sin\varphi}{\lambda - \overline{z^2}} \qquad \text{if } \lambda \neq \overline{z^2} \tag{B2}$$

However, problems arise if both numerator and denominator in these expressions have zero values at the same time. The correct values will then be obtained after following the next "exceptions" algorithms. If only a zero value in the denominator occurs, a value of $^1/_2\pi$ has to be assigned to the concerning angle. The correct value for tg φ is selected from

$$\text{if } \overline{xz} \neq 0 \text{ or } \overline{yz} \neq 0 \text{ then} \tag{B3}$$

$$\text{if } \overline{xy} = 0 \text{ or } \lambda = \overline{z^2} \text{ then } \text{tg}\,\varphi = -\frac{\overline{xz}}{\overline{yz}}$$

$$\text{else} \qquad \text{tg}\,\varphi = \frac{\overline{xz}}{\overline{yz}}$$

$$\text{else} \qquad \text{tg}\,\varphi = \frac{\lambda - \overline{x^2}}{\overline{xy}}$$

The calculation of tg θ gives problems if $\lambda = \overline{z^2}$ is combined with a zero numerator value; then its value is selected from

$$\text{if } \overline{yz} \neq 0 \text{ then} \qquad \text{tg}\,\theta = -\frac{\overline{xy}\cos\varphi + (\overline{y^2} - \lambda)\sin\varphi}{\overline{yz}} \tag{B4}$$

$$\text{else} \qquad \text{if } \overline{xz} \neq 0 \text{ then}$$

$$\text{tg}\,\theta = -\frac{(\overline{x^2} - \lambda)\cos\varphi + \overline{xy}\sin\varphi}{\overline{xz}}$$

$$\text{else} \qquad \text{tg}\,\theta = \infty \text{ (trivial case, gives unit vector)}$$

In the case of multiple eigenvalues, which is very unlikely,[18,21] a Gram−Schmidt method to complete the set of eigenvector(s) can be used.

More information about this method is available at the following address: Ir. H. W. H. M. Janszen, University of Twente, Faculty of Chemical Technology, CT 2362, P.O. Box 217, 7500 AE Enschede, The Netherlands, or E-mail: H.W.H.M.Janszen@ct.utwente.nl.

References and Notes

(1) Rubin, R. J.; Mazur, J. *Macromolecules* **1977**, *10*, 139.
(2) Kranbuehl, D. E.; Verdier, P. H.; Spencer, J. *J. Chem. Phys.* **1973**, *59*, 3861.
(3) Šolc, K.; Stockmayer, W. H. *J. Chem. Phys.* **1971**, *54*, 2756.
(4) Zimm, B. H. *Macromolecules* **1980**, *13*, 592.
(5) Debye, P.; Bueche, F. *J. Chem. Phys.* **1952**, *20*, 1337.
(6) Debye, P. *J. Chem. Phys.* **1946**, *14*, 636.
(7) Yamakawa. *Modern Theory of Polymer Solutions*; Harper & Row: New York, 1971, Chapter II.7.
(8) Flory, P. J. *Principles of Polymer Chemistry*; Cornell University Press: Ithaca, NY, 1953; Chapters VII.1, XII.2.
(9) Flory, P. J. *Statistical Mechanics of Chain Molecules*; Interscience: New York, 1969, reprint 1989; Chapter VIII.
(10) Fixman, M. *J. Chem. Phys.* **1962**, *36*, 306.
(11) Forsman, W. C. *J. Chem. Phys.* **1963**, *38*, 2118.
(12) Forsman, W. C. *J. Chem. Phys.* **1965**, *42*, 2829.
(13) Forsman, W. C. *J. Chem. Phys.* **1966**, *44*, 1716.
(14) Hoffman, R. F.; Forsman, W. C. *J. Chem. Phys.* **1969**, *50*, 2316.
(15) Kuhn, W. *Kolloïd.-Z.* **1934**, *68*, 2.
(16) Šolc, K. *J. Chem. Phys.* **1971**, *55*, 335.
(17) Šolc, K. *Polym. News* **1977**, *4*, 67.
(18) Eichinger, B. E. *Macromolecules* **1977**, *10*, 671.
(19) Eichinger, B. E. *Macromolecules* **1985**, *18*, 211.
(20) Gobush, W.; Šolc, K.; Stockmayer, W. H. *J. Chem. Phys.* **1974**, *60*, 12.
(21) Wei, G.; Eichinger, B. E. *Macromolecules* **1990**, *23*, 4845.
(22) Rudnick, J.; Gaspari, G. *Science* **1987**, *237*, 384.
(23) Bendler, J.; Šolc, K.; Gobush, W. *Macromolecules* **1977**, *10*, 635.
(24) (a) Tanaka, T.; Kotaka, T.; Inagaki, H. *Macromolecules* **1976**, *9*, 561. (b) Tanaka, T.; Kotaka, T.; Ban, K.; Hattori, M.; Inagaki, H. *Macromolecules* **1977**, *10*, 960.
(25) Birshtein, T. M.; Skvortsov, A. M.; Sariban, A. A. *Macromolecules* **1976**, *9*, 888.
(26) Pouchlý, J.; Zivný, A.; Sikora, A. *J. Polym. Sci., Polym. Phys. Ed.* **1972**, *10*, 151.
(27) Pouchlý, J.; Zivný, A.; Sikora, A. *J. Polym. Sci., Part C* **1972**, *39*, 133.
(28) Reference 9, Chapter I.2, pp 7−8.
(29) Theodorou, D. N.; Suter, U. W. *Macromolecules* **1985**, *18*, 1206.
(30) Reference 9; Chapter III and following.
(31) Bassler, K. E.; Olvera de la Cruz, M. *J. Phys. I Fr.* **1993**, *3*, 2387.
(32) Rubinstein, R. Y. *Simulation and the Monte Carlo Method*; John Wiley and Sons: New York, 1981; Chapter 2.3.2.
(33) (a) Box, G. E. P.; Muller, M. E. *Ann. Math. Stat.* **1958**, *29*, 610. (b) von Neumann, J. *Various Techniques Used in Connection with Random Digits*; U.S. National Bureau of Standards Applied Math Series No. 12; U.S. NBS: Washington, DC, 1959; pp 36. (c) Bell, J. R. Algorithm 334, Normal random deviates. *Commun. ACM* **1968**, *11* (7), 498. (d) Muller, M. E. A Note on a method for generating points uniformly on N-dimensional spheres. *Commun. ACM* **1959**, *2*, 19−20. (e) Muller, M. E.; A Comparison of Methods for Generating Normal Deviates on Digital Computers. *J. ACM* **1959**, *6*, 376.
(34) Hammersley, J. M.; Handscomb, D. C. *Monte Carlo Methods*; Methuen & Co.: London, 1964, Chapter 5.2.
(35) Binder, K.; Heermann, D. W. *Monte Carlo Simulation in Statistical Physics*; Springer Verlag: Berlin, 1988; Chapter 2.2.
(36) Rubin, R. J.; Mazur, J. *J. Chem. Phys.* **1975**, *63*, 5362.
(37) Koyama, R. *J. Phys. Soc. Jpn.* **1968**, *24*, 580.
(38) Volkenstein, M. V. *Configurational Statistics of Polymeric Chains*; Interscience: New York, 1963; Chapter 4.22, p 174.
(39) Bendler, J.; Šolc, K. *Polym. Eng. Sci.* **1977**, *17*, 622.
(40) Referee's note.

MA951114B